Volume 3 | Number 21 | 7 June 2015 | Pages 5357–5604

Journal of Materials Chemistry C

Materials for optical, magnetic and electronic devices

www.rsc.org/MaterialsC

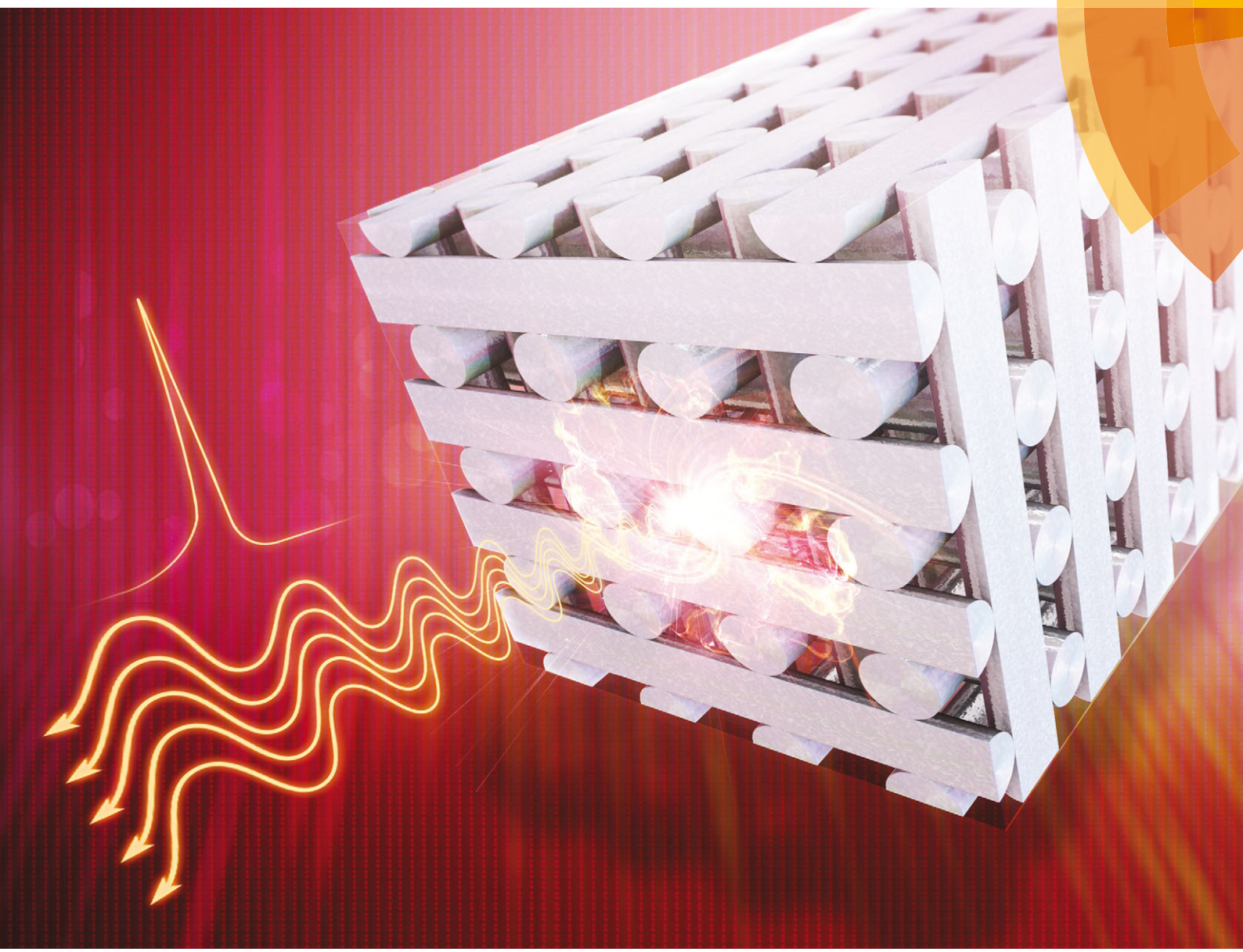

ISSN 2050-7526

ROYAL SOCIETY OF CHEMISTRY

PAPER

Myoung Hoon Song, Suk-Won Choi *et al.*

A well-aligned simple cubic blue phase for a liquid crystal laser

Journal of Materials Chemistry C

PAPER

View Article Online
View Journal | View Issue

Cite this: J. Mater. Chem. C, 2015, 3, 5383

Received 12th February 2015,
Accepted 10th March 2015

DOI: 10.1039/c5tc00420a

www.rsc.org/MaterialsC

A well-aligned simple cubic blue phase for a liquid crystal laser

Kibeom Kim,†[a] Sung-Taek Hur,†[a] Sunhwan Kim,[a] Seong-Yong Jo,[a] Bo Ram Lee,[b] Myoung Hoon Song*[b] and Suk-Won Choi*[a]

Here, a well-aligned dye-doped simple cubic blue phase (BPII) sample is fabricated that is stable over the temperature range of 4 °C and has a photonic bandgap (PBG) equivalent to a visible optical wavelength. We demonstrate the maximum widest tunability range of 30 nm as a function of temperature for the well-aligned dye-doped BPII sample. Moreover, it is found that the emission threshold energy for the laser action can be dramatically reduced.

Introduction

The primary advantages of liquid crystals (LCs) over photonic crystals (PCs) are that periodic structures of LCs assemble spontaneously without the need for complex manufacturing processes; these soft matter can then be easily deformed to achieve facile wavelength tuning.[1] Of the various types of soft liquid crystalline substances, cubic blue phases (BPs) are intriguing because they organize spontaneously into three-dimensional (3D) cubic structures with lattice periods of a few hundred nm.[2] This self-organized structures give a photonic bandgap (PBG) for visible light. Thus, cubic BP materials can be regarded as a type of PC, and have attracted much attention due to their ability to control the propagation of light in different frequency ranges.[1]

Cubic BPs can be classified into two types, namely, body-centered cubic BP (BPI) and simple cubic BP (BPII), in order of increasing temperature from the low-temperature chiral nematic (N*) to the high-temperature isotropic phase.[3,4] As a result of this unique PC property, lasing phenomena at the PBG edge of cubic BPs are of considerable interest. Because photons generated from a gain medium (dyes) with appropriate fluorescence properties are suppressed and experience long dwell-times inside the PBG, the formation of a mirror-less BP laser can be expected.[1,5] In actuality, lasing phenomena have been demonstrated using both a polymer-stabilized BPI[2] and a wide-temperature BPI.[6,7] Recently, a widely tunable lasing peak shift of more than 100 nm was obtained using cubic BPI in a mixed system of conventional rod-like and unusual bent-core nematogens blended with a chiral dopant.[8] It is worth noting that, although laser emission in three orthogonal directions by means of the 3D PBG structure using cubic BPII was reported by Cao *et al.* in 2002,[9] to date, most lasing phenomena have been demonstrated using BPI. This is because BPII is stable in an extremely narrow temperature range only (typically 0–1 °C),[3] which limits their applicability as PCs.

Typically, liquid crystalline BPs exhibit multi-platelet domains when placed between two glass substrates. Thus, the relative Bragg reflection intensities resulting from a specific plane of the cubic BP structure inevitably deteriorate. Although the excitation threshold energy is expected to be lower than that of a corresponding cholesteric phase under similar experimental conditions,[1] it is difficult to obtain high reflection (gain) with low lasing threshold in a conventional BP laser system, because of the abovementioned deteriorated Bragg reflection. A relatively high and constant reflection intensity, originating from a specific plane of the BP structure, is desirable for the realization of a high performance mirror-less liquid crystalline BP laser. Thus, preparation of a uniform single-color monodomain BP is indispensable from an application viewpoint. Although several studies on a monodomain BP have been reported,[10,11] it is known that controlling BP orientation is extremely difficult in general, since its direction is not uniform, unlike that of nematic (N) LCs.[12] However, the previously described difficulty in orientation control has been primarily demonstrated using BPI, as a result of the limited stability of BPII (within the typical narrow temperature range of 0–1 °C). Recently, BPII exhibiting relatively wide temperature ranges (~4 °C) has been reported, and several systematic investigations of BPII have been conducted.[3,13] More recently, several researchers have demonstrated that uniform and monodomain-like liquid crystalline BP covering the entire area of a fabricated cell can be easily realized by means of a conventional

[a] Department of Advanced Materials Engineering for Information and Electronics, Kyung Hee University, Yongin-shi, Gyeonggi-do 446-701, Korea. E-mail: schoi@khu.ac.kr
[b] School of Materials Science Engineering/KIST-UNIST Ulsan Center for Convergent Materials/Low Dimensional Carbon Materials Center, Ulsan National Institute of Science and Technology (UNIST), UNIST-gil 50, Ulsan 689-798, Korea. E-mail: mhsong@unist.ac.kr
† The first two authors contributed equally to this work.

surface rubbing treatment.[13,14] Thus, it can be expected that this uniform BPII with mono-platelet domains realizes a lower lasing threshold because of its high and constant Bragg reflection.

In the present work, we fabricate a dye-doped cubic BPII sample that exhibits wide temperature stability with a PBG equivalent to a visible optical wavelength, and then successfully prepare well-aligned cubic BPII with mono-platelet domains using a conventional rubbing treatment on glass surfaces. Using this system, we demonstrate the maximum widest tunability range of 30 nm as a function of temperature in the well-aligned dye-doped BPII sample. To the best of our knowledge, the tunability of the lasing wavelength in BPII systems has not yet been demonstrated. Moreover, we are able to dramatically reduce the emission threshold energy for the laser action. Ultimately, this study proposes and supports the feasibility of LC BPII for use in PC applications.

Experimental

Materials

In order to obtain cubic BPII, we prepared a host nematic liquid crystal (NLC) mixture consisting of a rod-like nematogen (80 wt%) and a bent-core molecule A (BC-A, 20 wt%).[15] The rod-like nematogen (MLC-7026-000, Merck Co.) used here was a commercially available multi-component mixture with negative dielectric anisotropy ($\Delta\varepsilon = -3.7$ at 25 °C, 1.0 kHz). By means of blending the chiral dopant (6 wt%, ISO–(6OBA)$_2$)[16] with the host N mixture, a host N* mixture was prepared. LC BPs appeared between the N* and isotropic phase in the prepared host N* mixture in order of increasing temperature, and the chemical structures of the bent-core molecule and chiral dopant are shown in Fig. 1.

The dye-doped cubic BPs were prepared as follows: as a gain medium, a commercialized dye was added to the host N* mixture (0.2 wt% pyrromethene 597, Exciton). This laser dye exhibits high photon efficiency, is well-soluble, and had little effect on the expected phase sequences of our liquid crystalline phases.[8] The typical absorption and emission spectra of the gain medium are depicted in Fig. 2. Thus, the laser dye, pyrromethene 597, covers the green-red wavelength range. The chemical structure of pyrromethene 597 is also shown in the inset of Fig. 2.

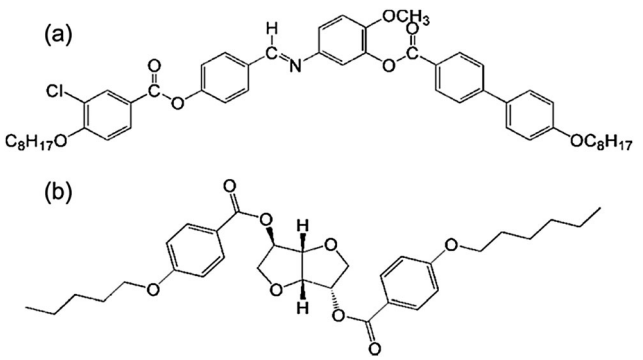

Fig. 1 Chemical structures of the (a) bent-core molecules and (b) chiral dopants used in this work.

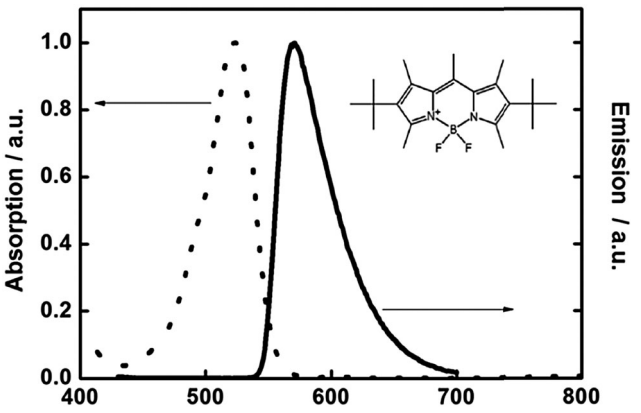

Fig. 2 Typical absorption (dashed line) and emission (solid line) spectra of pyrromethene 597. Chemical structure of pyrromethene 597 (inset).

Cell fabrication

We fabricated two types of sandwiched cells with cell gaps of 20 μm: (1) a pair of slides with no surface treatment (Cell-1), and (2) a pair of slides having undergone surface rubbing treatment (Cell-2). The sandwiched cells undergoing rubbing treatment were prepared as follows: a commercially available polyimide (PI) (AL22620, JSR) was spin-coated on the slides, which were then cured at 180 °C for 20 min. Then, rubbing was performed using a commercial rubbing machine with velvet at a moderate rubbing strength. Two slides were assembled at antiparallel rubbing directions (relative to each other) and the prepared mixtures were injected into both Cell-1 and Cell-2.

Lasing setup

The setup for laser emission is described in ref. 8. A 530 nm pulsed laser beam from an optical parametric oscillator, pumped using second harmonic light from a Nd:YAG laser, was employed as an optical pumping source. The pulse width and the repetition frequency were 6 ns and 10 Hz, respectively. The laser beam was focused on the sample surface (the spot size of the pumping beam was approximately 150 μm) at an oblique incidence (approximately 45°). The output lasing emission in the forward direction of the sample was collected using a multi-channel spectrometer (USB 4000, Ocean Optics).

Results and discussion

Fig. 3(a) illustrates a sequence of typical polarized optical microscopy (POM) images, revealing the textures of our chiral mixture blended with 6.2 wt% chiral dopant in Cell-2. Once the cells had cooled from the isotropic to the N* phase, POM images were carefully recorded during a heating process. Upon heating at a rate of 0.1 °C min^{-1}, the N* phase (at 71 °C) with oily streaks changed to a greenish fluid phase (at 71.2 °C). This greenish phase then gradually changed to a reddish phase in response to the increasing temperature. Upon further heating, the reddish phase progressed to the isotropic phase (75.5 °C). Because the phases exhibiting colors appeared between the N* and isotropic phases, the phase observed here must be LC BP. However, the observed phase has

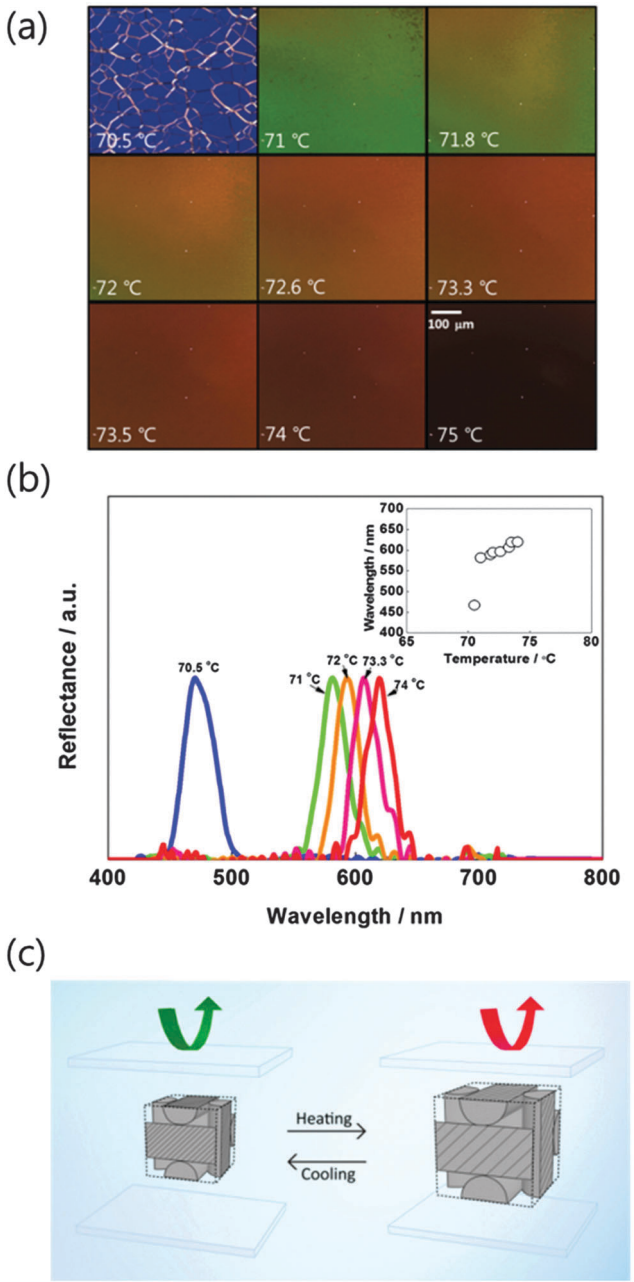

Fig. 3 (a) Typical POM images revealing the textures of the chiral mixture blended with 6.2 wt% chiral dopant in Cell-2. (b) Temperature dependence of the Bragg reflection wavelength during heating. Central wavelength of the Bragg reflection band during heating (inset). (c) Schematic illustration of the Bragg reflection of the BPII under thermal stimuli.

none of the platelet textures which are usually observed in BPs. Therefore, it was confirmed that BP with mono-domain textures possessing a uniformly oriented lattice plane was realized in the sandwich cell subjected to the rubbing treatment. Although some areas with non-uniform color were also observed in the cell, an entirely uniform BP domain that grew to a size of over 500 μm could be realized. The non-uniform area could also be improved through repeated cooling and heating cycles over the BP temperature ranges with a rate of 0.1 °C min^{-1}.

The question can then be posed as to whether this phase is BPI or BPII. In order to respond to this question, the temperature dependence of the Bragg reflection wavelength during heating (0.1 °C min^{-1}) was recorded, as shown in Fig. 3(b). The central wavelength of the Bragg reflection band during heating is also visible in the inset. Fig. 3(b) clearly shows a discontinuous change in the temperature dependence of the Bragg reflection wavelength at the N*–BP transition at heating temperatures >71 °C. From POM and Bragg reflection observations, the observed color in the cubic BP region gradually changed from a short to a long wavelength with increasing temperature. This trend strongly suggests that this phase corresponds to liquid crystalline BPII.[3,17,18] Typically, BPI gradually changes from a long to a short wavelength with increasing temperature, while the opposite is observed for BPII. Overall, the PBG of our BPII changed by approximately 40 nm in the temperature range of about 4 °C. This shift was found to be reversible for repeated temperature cycles between 71.2 and 75 °C, which means that the size of the BP lattice was enlarged (reduced) and, thus, the corresponding PBG moved towards a longer (shorter) wavelength with increasing (decreasing) temperature, as illustrated in Fig. 3(c).

Furthermore, it was confirmed that we could fabricate a mono-domain cubic BPII with a uniformly oriented (100) lattice plane in a sandwich cell subjected to a rubbing treatment. In general, rubbing treatments had little influence on the BPI alignment in our previous study, because its direction is not uniform, unlike that of NLCs. Interestingly, in this study (featuring BPII), the rubbing treatment easily created a monodomain-like BPII with a uniformly aligned periodic lattice plane (100). Surprisingly, the obtained uniform domain covered the entire region of fabricated cells. It is likely that the alignment of the lattice plane of a cubic BPII is easier to achieve than that of a cubic BPI. On a side note, we also attempted to fabricate mono-domain cubic BPII in several sandwich cells subjected to the rubbing treatment using other commercially available PIs. The BPII has a tendency to be well-aligned following the rubbing treatment, irrespective of the specific PIs used. This is because BPII has simple cubic symmetry and, unlike BPI, the defect lines characterizing its equilibrium structure are not separated and, in fact, intersect. We believe that this topological difference is responsible for the difference in alignment between BPII and BPI.[19]

From the POM and Bragg reflection observations, it was established that only BPII was observed in our case and, as stated above, the evaluated temperature range of the BPII was approximately 4 °C during heating, which is much wider than those of conventional nematogens blended with chiral dopants. However, the observed temperature range may be relatively narrow with regard to mixed systems of conventional rod-like nematogens and unusual bent-core molecules blended with chiral dopants.[8,20–23] In our previous work, a BPI with a wide temperature range of 25 °C was realized in a mixed system of a conventional rod-like nematogen and BC-A blended with chiral dopants.[8] In contrast, a cubic BPII with a temperature interval of 4 °C was observed in the mixed system of the present work, consisting of a rod-like nematogen and BC-A blended with chiral dopants.

The BC-A and chiral dopant used in both the previous and present cases were the same. However, in the previous case, a conventional rod-like nematogen with positive dielectric anisotropy was employed, while a rod-like nematogen with negative dielectric anisotropy was used in this work. We doubt that the differences in the observed BPs and temperature range depend on the dielectric properties of the host rod-like nematogen, but additional details on the above relationship will be reported in a future study.

Next, lasing action based on the photonic effect in our cubic BPII was investigated. Two kinds of sandwiched cells were prepared, and both Cell-1 and Cell-2 were filled with the dye-doped cubic BPII. Fig. 4(a) and (b) show typical reflectance of the lattice plane (100) and emission spectra of Cell-1 and Cell-2, respectively. In addition, typical POM images are visible in the inset. It was found that the PBG originating from the periodic lattice plane (100) was insufficient, because the lattice planes were not perfectly aligned in Cell-1. The relative Bragg reflection intensities resulting from their periodic structures were determined based on the lattice plane orientation distributions of the different platelet domains, which vary between samples. In actuality, although multi-reflection colors due to several periodic lattice planes were observed in the POM image for Cell-1, the relative Bragg reflection intensities were too small to produce precise Bragg reflection at wavelengths that were detectable using our experimental setup. In contrast, the Bragg reflection originating from the periodic lattice plane (100) in Cell-2 was relatively high and constant as a result of the rubbing treatment. While a blunt emission peak with a full width at half maximum (FWHM) of approximately 4.5 nm appeared for Cell-1, a narrow and sharp peak with a FWHM in the region of 1.2 nm appeared for Cell-2, just in the higher energy range of the PBG. This observation distinctly proves that the laser emission described above is due to the band edge mode.[1]

Typical laser emission spectra at elevated temperatures for Cell-2 are shown in Fig. 5(a), while peak lasing wavelengths collected at different temperatures for Cell-2 are visible in the inset. When the temperature of Cell-2 increased from 71.2–75 °C, the laser peak shifted 30 nm towards longer wavelengths, from roughly 580–610 nm. To date, such a wide shift in the lasing peak for a dye-doped cubic BPII has not been reported. Furthermore, this shift in lasing wavelength was reversible for repeated temperature cycles between 71.2 and 75 °C, as illustrated in Fig. 5(b). Note that the lasing intensity decreased slightly with increasing temperature, because the lasing intensity primarily depends on the PBG of BPII and the emission band of the doped dye used in this work.

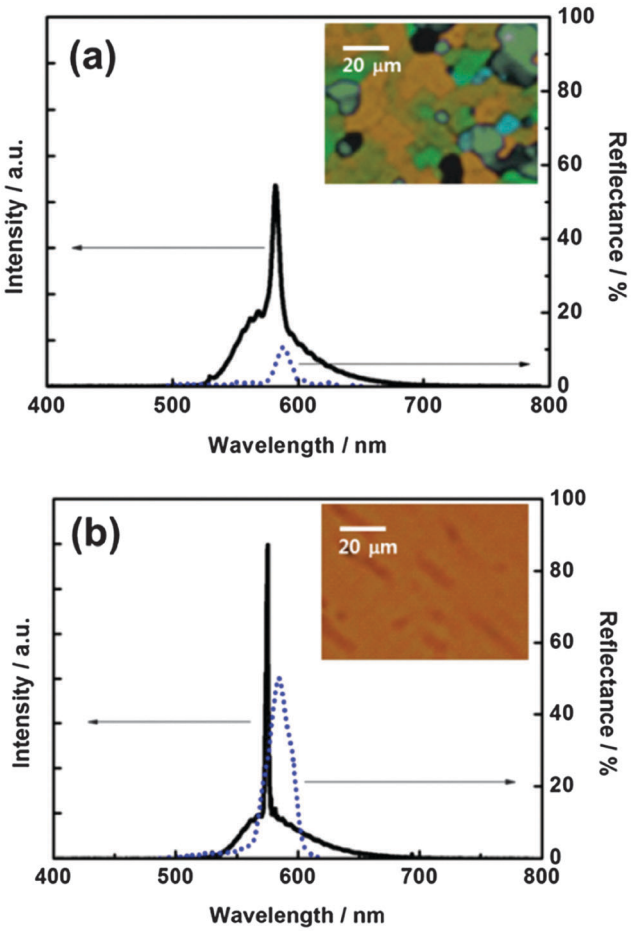

Fig. 4 Typical reflectance due to the lattice plane (100) and emission spectra of (a) Cell-1 and (b) Cell-2. Typical POM images (inset).

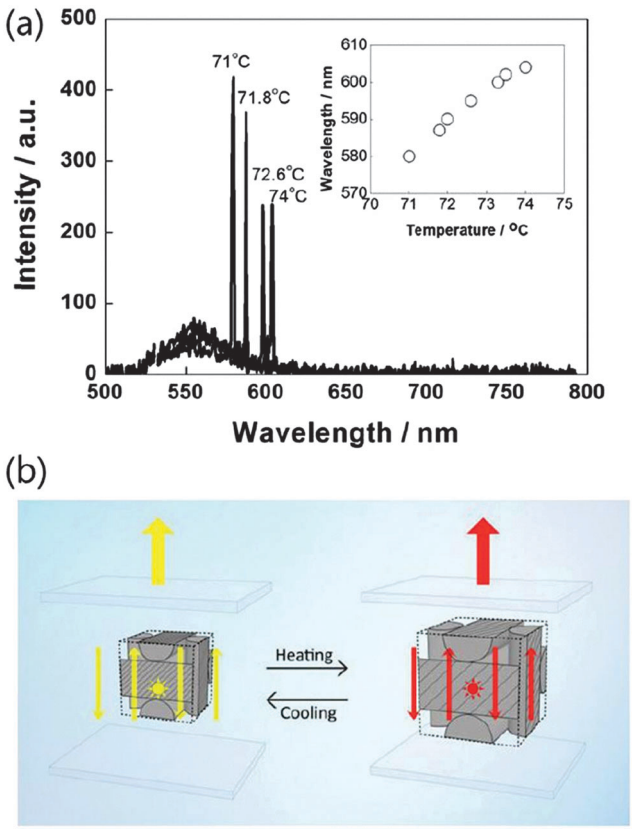

Fig. 5 (a) Typical laser emission spectra at elevated temperatures for Cell-2. Peak lasing wavelengths collected at different temperatures (inset). (b) Schematic illustration of BPII laser tuning under thermal stimuli.

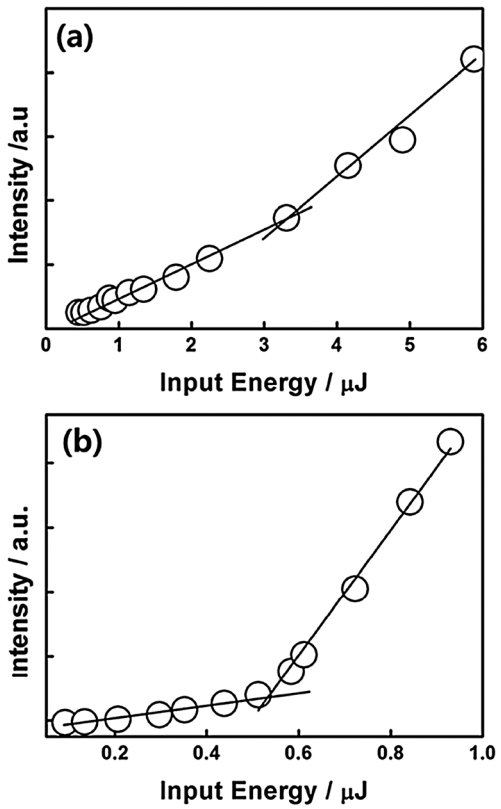

Fig. 6 Typical threshold behavior of (a) Cell-1 and (b) Cell-2.

Fig. 6(a) and (b) show the typical threshold behavior of Cell-1 and Cell-2. The typical threshold value for Cell-1 was found to be approximately 3.3 μJ per pulse, corresponding to an energy-per-excited-area of approximately 15 mJ cm^{-2}. This energy value is typical for lasing in the dye-doped BPs composed of multi-platelets that are usually observed in liquid crystalline BPs.[1,6,24] Interestingly, the emission threshold energy can be dramatically reduced through the fabrication of the mono-domain cubic BPII. The typical threshold value of Cell-2 was found to be approximately 0.53 μJ per pulse, which is about 1/6 times less than that of Cell-1. In addition, the observed threshold value was almost constant, irrespective of the temperature. In a well-aligned BPII system, it is easy to obtain relatively high gain with low threshold for lasing because of the high and constant Bragg reflection. Hence, well-aligned BPII materials may hold promise as laser media based on the photonic effect.

Conclusions

Of the various topics related to cubic BPs, lasing phenomena at the PBG edge have been receiving particular attention. Liquid crystalline cubic BPs are divided into two types (body-centered BPI and simple cubic BPII). To date, a number of studies have been conducted on the laser emission of BPI, but the lasing properties of BPII have been neglected as a result of their limited stability in the narrow temperature range. Here, we have fabricated a well-aligned liquid crystalline BPII that is stable over the temperature range of approximately 4 °C, for which a wide range in PBG shift (over 40 nm) was observed. The lasing action based on the band edge mode occurs at the PBG with the cubic BPII's self-assembled periodicity, and the lasing wavelength is tuned by varying the temperature. We have dramatically reduced the emission threshold energy for the laser action using the well-aligned cubic BPII, and a lasing peak shift of approximately 30 nm has been achieved due to the large shift for PBG. As a result, this study establishes the feasibility of using cubic BPII in PC applications. However, the temperature range of the BPII examined in this work is still narrow and limits its practical application. In order to further expand the BPII temperature range, we will now investigate polymer-stabilized BPII.

Acknowledgements

This work was supported by the Basic Science Research Program (NRF-2013R1A1A2061996) and the Mid-Career Researcher Program (NRF-2012R1A2A2A06046931), through the National Research Foundation of Korea (NRF), funded by the Ministry of Science, ICT & Future Planning (MSIP).

Notes and references

1 H. J. Coles and S. M. Morris, *Nat. Photonics*, 2010, **4**, 676.
2 S. Yokoyama, S. Mashiko, H. Kikuchi, K. Uchida and T. Nagamura, *Adv. Mater.*, 2006, **18**, 48.
3 K.-W. Park, M.-J. Gim, S. Kim, S.-T. Hur and S.-W. Choi, *ACS Appl. Mater. Interfaces*, 2013, **5**, 8025.
4 T.-H. Lin, Y. Li, C.-T. Wang, H.-C. Jau, C.-W. Chen, C.-C. Li, H. K. Bisoyi, T. J. Bunnig and Q. Li, *Adv. Mater.*, 2013, **25**, 5050.
5 Y. Inoue, H. Yoshida, K. Inoue, Y. Shiozaki, H. Kubo, A. Fujii and M. Ozaki, *Adv. Mater.*, 2011, **23**, 5498.
6 S. M. Morris, A. D. Ford, C. Gillespie, M. N. Pivnenko, O. Hadeler and H. J. Coles, *J. Soc. Inf. Disp.*, 2006, **14**, 565.
7 F. Castles, F. V. Day, S. M. Morris, D.-H. Ko, D. J. Gardiner, M. M. Qasim, S. Nosheen, P. J. W. Hands, S. S. Choi, R. H. Friend and H. J. Coles, *Nat. Mater.*, 2012, **11**, 599.
8 S.-T. Hur, B. R. Lee, M.-J. Gim, K.-W. Park, M. H. Song and S.-W. Choi, *Adv. Mater.*, 2013, **25**, 3002.
9 W. Y. Cao, A. Munoz, P. Palffy-Muhoray and B. Taheri, *Nat. Mater.*, 2002, **1**, 111.
10 J. Yan, S.-T. Wu, K.-L. Cheng and J.-W. Shiu, *Appl. Phys. Lett.*, 2013, **102**, 081102.
11 P. Nayek, H. Jeong, H. R. Park, S.-W. Kang, S. H. Lee, H. S. Park, H. J. Lee and H. S. Kim, *Appl. Phys. Express*, 2012, **5**, 051701.
12 S.-I. Yamamoto, Y. Haseba, H. Higuchi, Y. Okumura and H. Kikuchi, *Liq. Cryst.*, 2013, **40**, 639.
13 K. Kim, S. Kim, S.-W. Choi, *The 2nd Asia Conference on Liquid Crystals*, Busan, Korea (Jan. 19–21, 2015).
14 H. Yoshida, K. Anucha, Y. Kawata, S. Tanaka, M. Ozaki, *The 2nd Asia Conference on Liquid Crystals, Busan, Korea* (Jan. 19–21, 2015).

15 T. Niori, J. Yamamoto and H. Yokoyama, *Mol. Cryst. Liq. Cryst.*, 2004, **409**, 475–482.
16 T. Iwata, K. Suzuki, H. Higuchi and H. Kikuchi, *Liq. Cryst.*, 2009, **36**, 947.
17 H. J. Coles and M. N. Pivnenko, *Nature*, 2005, **436**, 997.
18 H. Choi, H. Higuchi and H. Kikuchi, *Appl. Phys. Lett.*, 2011, **98**, 131905.
19 O. Henrich, K. Stratford, P. V. Coveney, M. E. Cates and D. Marenduzzo, *Soft Matter*, 2013, **9**, 10243.
20 M. Lee, S.-T. Hur, H. Higuchi, K. Song, S.-W. Choi and H. Kikuchi, *J. Mater. Chem.*, 2010, **20**, 5813.
21 S.-T. Hur, M.-J. Gim, H.-J. Yoo, S.-W. Choi and H. Takezoe, *Soft Matter*, 2011, **7**, 8800.
22 M.-J. Gim, S.-T. Hur, K.-W. Park, M. Lee, S.-W. Choi and H. Takezoe, *Chem. Commun.*, 2012, **48**, 9968.
23 M.-J. Gim, K.-Y. Park and S.-W. Choi, *Opt. Mater.*, 2013, **36**, 414.
24 A. Mazzulla, G. Petriashvili, M. A. Matranga, M. P. D. Santo and R. Barberi, *Soft Matter*, 2012, **8**, 4882.